

Influence of Hydroxyapatite-Coated and Growth Factor–Releasing Interference Screws on Tendon–Bone Healing in an Ovine Model

Yan Lu, M.D., Mark D. Markel, D.V.M., Ph.D., Brett Nemke, B.S., J. Sam Lee, Ph.D., Ben K. Graf, M.D., and William L. Murphy, Ph.D.

Purpose: Our purpose was to determine whether a bioresorbable interference screw coated with a hydroxyapatite-based mineral layer designed to release an engineered peptide growth factor (linkBMP-2 [where “BMP-2” indicates bone morphogenetic protein 2]) improved tendon–bone healing compared with a screw without coating. **Methods:** Tagged linkBMP-2 peptides were used to quantify binding efficiency and release kinetics on 9 mineral-coated BIORCI screws (Smith & Nephew, Andover, MA). Fourteen mature female sheep were used in this study. In each of the 14 sheep, each stifle was randomized to either receive a linkBMP-2–coated or uncoated interference screw ($n = 14$ per treatment). The sheep were euthanized at 6 weeks after surgery. Eight sheep were subjected to biomechanical testing for peak load at failure and stiffness, and six sheep were used for histologic analysis according to a semiquantitative scoring scale. **Results:** The linkBMP-2 molecule bound efficiently to the surface of mineral-coated interference screws. Over 80% of the initially bound linkBMP-2 was released during a 6-week time frame in vitro. Peak load at failure in the linkBMP-2–coated interference screw group (mean \pm SD, 449.3 ± 84.7 N) was not significantly different from that in the uncoated group (421.0 ± 61.8 N) ($P = .22$). Stiffness in the linkBMP-2–coated interference screw group (157.3 ± 39.6 N/mm) was not significantly different from that in the uncoated group (140.6 ± 20.3 N/mm) ($P = .12$). Histologic analysis showed that the tendons in the linkBMP-2–coated interference screw group had higher scores (better) than the uncoated group. In the linkBMP-2–coated interference screw group, mesenchymal cells were present at the interface between screw and tendon, whereas these cells were not present in the uncoated group. **Conclusions:** We found that linkBMP-2 can be bound onto a mineral-coated BIORCI interference screw surface and subsequently released from the screw surface in a sustained manner. The histologic result of this study showed that the linkBMP-2–coated interference screw significantly improved the histologic scores of early tendon–bone healing in this sheep model. **Clinical Relevance:** This linkBMP-2 coating material may improve early tendon/ligament fixation. **Key Words:** rhBMP-2—ACL—Tendon–bone healing—Growth factors—Interference screw—Sheep.

From the Comparative Orthopaedic Research Laboratory, School of Veterinary Medicine (Y.L., M.D.M., B.N.), and Departments of Biomedical Engineering (J.S.L., W.L.M.), Pharmacology (W.L.M.), and Orthopedics and Rehabilitation (Y.L., B.K.G.), University of Wisconsin–Madison, Madison, Wisconsin, U.S.A.

Supported by the Wallace H. Coulter Foundation (Translational Research Partnership Grant) and the National Institutes of Health (R03AR052893). The authors report no conflict of interest.

Received November 13, 2008; accepted June 10, 2009.

Address correspondence and reprint requests to Yan Lu, M.D., Comparative Orthopaedic Research Laboratory, Department of Medical Sciences, School of Veterinary Medicine, University of Wisconsin–Madison, 2015 Linden Dr, Madison, WI 53706-1102, U.S.A. E-mail: luy@svm.vetmed.wisc.edu

© 2009 by the Arthroscopy Association of North America

0749-8063/09/2512-8636\$36.00/0

doi:10.1016/j.arthro.2009.06.008

Note: To access the supplementary tables accompanying this report, visit the December issue of *Arthroscopy* at www.arthroscopyjournal.org.

Currently, tendon grafts plus biodegradable interference screws transplanted into bone tunnels are widely used for anterior cruciate ligament (ACL) reconstruction. An interference screw can mechanically fix the tendon graft against one side of the bone tunnel wall and place tendon and bone in close contact.¹⁻³ However, interference screw fixation can potentially damage the tendon graft at the time of screw insertion, and the tendon-bone contact area is limited within the tunnel.^{4,5} Another problem with existing interference screws is that they may exert too much pressure on the graft within the cancellous bone regions or, alternatively, exert too little pressure on the graft within the cortical bone regions, potentially resulting in insufficient holding strength for securing the graft in place.⁶ In addition, inadequate fixation and inflammatory reactions after partial degradation of interference screws may occur.⁷ Taken together, these factors may significantly hinder tendon-bone healing after reconstruction surgery. A previous study has reported that, in the femur, fixation of tendon grafts with interference screws provided adequate strength for early rehabilitation, but the adequacy of interference screw fixation in the tibia remains a question.⁸

Multiple investigators have reported application of biologic agents to improve tendon-bone healing after ACL reconstruction surgery.⁹⁻¹¹ Rodeo et al.¹¹ reported improved bone formation around a tendon graft in an extra-articular bone tunnel in a canine model using exogenous recombinant human bone morphogenetic protein 2 (BMP-2). Anderson et al.⁹ showed improved healing by applying a mixture of bone-derived growth factors at the tendon-bone interface in a rabbit ACL reconstruction model. Martinek et al.¹⁰ showed that BMP-2 gene delivery using an adenoviral vector significantly improved tendon-bone healing in a rabbit model. These studies show that growth factors, particularly BMP-2, can improve tendon-bone healing in ACL reconstruction models.

A significant challenge limiting the use of biologics (e.g., growth factors) in ACL reconstruction is delivery. Recent studies have indicated that the release rate of bone morphogenetic proteins influences biological outcomes¹² and that short-term bolus delivery of BMP-2 may be less effective than sustained delivery in orthopaedic applications.¹³ In addition, delivery of large doses of BMP-2 can have deleterious effects such as hematoma at adjacent sites *in vivo*,¹⁴ so localized delivery is desirable. An additional challenge in growth factor delivery approaches is the inherent difficulty in combining a growth factor carrier material with other surgical components commonly used to

promote fixation, such as interference screws. The aforementioned studies have delivered growth factors using an absorbable type I collagen sponge as a carrier, which has been shown to release proteins over short time frames (hours to days) in a manner that may not be spatially localized.¹⁴ In addition, it may be practically difficult to combine collagen sponges with standard surgical components, such as interference screws used in ACL reconstruction. Therefore collagen sponges may not be an optimal carrier material for growth factor delivery in ACL reconstruction. The current challenges that complicate growth factor delivery call for an approach that allows for sustained, localized delivery from a carrier material that is integrated with other components of the surgical technique.

In this study we used a novel method to coat biodegradable interference screws with a hydroxyapatite-based mineral layer, which is designed to release an engineered peptide growth factor in a sustained manner. Some investigators have performed studies to determine the influence of implants coated with BMP-2 on osteointegration and fixation in animal models.¹⁵⁻¹⁷ The engineered growth factor, here termed "linkBMP-2," has 2 functional units: (1) an osteocalcin-inspired peptide sequence designed to bind to hydroxyapatite mineral surfaces and (2) a BMP-2-derived peptide sequence previously shown by Tanihara and coworkers¹⁸ to retain a portion of the biological activity of recombinant human BMP-2. The resulting linkBMP-2 growth factor is capable of binding to a hydroxyapatite mineral coating, which is grown on biodegradable BIORCI interference screws (Smith & Nephew, Andover, MA) by use of a well-defined approach developed previously.¹⁹⁻²¹

The purpose of this study was to determine whether a biodegradable interference screw coated with a mineral layer releasing linkBMP-2 would improve tendon-bone healing when compared with an uncoated screw. We hypothesized that the coated biodegradable interference screw would result in better biomechanical and histologic outcomes because of improved tendon-bone healing compared with an uncoated screw.

METHODS

All experimental protocols were approved by the Institutional Animal Use and Care Committee. Fourteen Hampshire mature female sheep, ranging in age from 2 to 5 years and weighing between 60 and 100 kg (mean \pm SD, 66.4 \pm 8.6 kg), were used in the study.

In each of the 14 sheep, one of the stifles was randomized (block design) to receive a coated interference screw and the other (contralateral) to receive an uncoated interference screw ($n = 14$ per treatment). "Coated" interference screws included a continuous hydroxyapatite mineral coating treated with the linkBMP-2 molecule as described later. The sheep were euthanized at 6 weeks after surgery. We used 8 sheep (16 stifles, 8 per group) for biomechanical testing and 6 sheep (12 stifles, 6 per group) for histologic analysis.

Mineral Coating of BIORCI Screw

A BIORCI screw composed of poly-L-lactide (Smith & Nephew) with a hydroxyapatite mineral layer grown on its surface by incubation in modified simulated body fluid (mSBF) was used in this study, as described elsewhere.¹⁹⁻²¹ In brief, screws were first immersed in 5 mL of 0.5-mol/L sodium hydroxide for 60 minutes to produce a hydrolyzed surface. The hydrolyzed screws were washed with distilled water (dH₂O) 5 times and then incubated in 20 mL of mSBF for 10 days for mineral growth. The solution was replaced with fresh mSBF daily to ensure adequate ion concentrations for mineral growth. The surface morphologies of mineral-coated and uncoated BIORCI screws were examined by scanning electron microscopy. A conductive gold coating was applied to the surface of a screw by sputter coating, and samples were imaged under high vacuum conditions by use of an LEO 1530 scanning electron microscope (Zeiss, Oberkochen, Germany) operating at 10 to 30 kV.

Fluorescently Tagged Peptide Binding and Release Kinetics

We used linkBMP-2 peptides tagged on their N terminus with 5(6)-FAM—5(6)-carboxyfluorescein (Anaspec, San José, CA) to quantify binding efficiency and release kinetics on 9 mineral-coated BIORCI screws. Various concentrations of fluorescently tagged peptides were dissolved in dH₂O (1 to 5 mg/mL) and were incubated with the mineral-coated BIORCI screws at 37°C for 4 hours with constant agitation. Peptide-containing solutions then were collected, and the peptide concentration remaining in solution was determined by absorbance at 405 nm. To measure release kinetics, mineral-coated screws were first incubated in 5 mg/mL of fluorescently tagged peptide and then incubated at 37°C with constant agitation. Solutions of released peptide were collected at indicated time durations (0, 0.5, 1, 2, 3, 4, 5, and 6 weeks). Peptide concentrations in release solutions were calculated by comparison to a standard curve

relating fluorescently labeled peptide concentration to fluorescence emission in solution.

Preparation of Coated BIORCI Screws for Implantation

We sterilized linkBMP-2 peptide and mSBF solutions by 0.2- μ L syringe filtering. The BIORCI screws were incubated in mSBF for 10 days to form a mineral coating and were then incubated for at least 4 hours in 5 mL of linkBMP-2 peptide solution (5 mg/mL in dH₂O) and directly used in surgery.

Surgical Procedure

An 8.0-cm arthrotomy was made on the lateral side of the femoropatellar joint, and the long digital extensor (LDE) tendon and proximal and lateral tibial metaphyses were exposed. The LDE tendon was then released from its attachment on the lateral femoral condyle as previously described.^{5,22}

For both coated and uncoated interference screw groups, the 20-mm length of tendon was measured and sutured with running and locking sutures by use of a nonabsorbable braided suture (No. 5 Ethibond; Ethicon, Somerville, NJ). The diameter of the tendon with the suture incorporated was measured with a custom-designed measuring device (Smith & Nephew). A 7- to 8-mm-diameter tunnel (based on the measurement of LDE tendon diameter with suture for each individual sheep), 25 mm in length, was drilled through the tibial metaphysis by use of a guidewire, starting just distal and lateral to the tibial tubercle below the groove for the digital extensor tendon and exiting on the medial side of the tibia. The tibial tunnels were drilled through the tibial metaphysis without interference with the stifle joint. A C-shaped drill guide was used for accurate and reproducible placement of the bone tunnel. The LDE tendon was passed through the drilled tunnel with the braided sutures so that 20 mm of tendon was inside the bone tunnel in each specimen. The 20-mm length of tendon in the tunnel was chosen based on a previously reported *in vivo* canine study.²³ The LDE tendon was then tied over a post screw (4.0-mm cancellous bone screw, 16 mm in length; Synthes Vet, West Chester, PA) with a washer on the medial side of the tibia with the sheep stifle in a neutral position (45° of flexion). A 7-mm screw tap was used to tap the tendon-bone tunnel to avoid damage to the coating during screw insertion. A BIORCI screw (7 mm in diameter and 25 mm in length; Smith & Nephew) coated with a mineral layer with linkBMP-2 or without coating was screwed into the bone tunnel

from the medial to the lateral direction. The stifle was then lavaged, and the incisions were closed routinely.

The sheep were allowed to bear weight immediately postoperatively and were examined for signs of incision swelling or other complications after surgery.

Biomechanical Testing

After 6 weeks, all sheep were euthanized for either biomechanical or histologic analyses. The tibiae were harvested with the attached LDE tendons. Eight paired stifles were randomly selected for mechanical testing. Before testing, the post screw and washer were removed so that the holding force of the interference screw and the biological healing of the tendon to bone could be measured. The interference screw was not removed to avoid damage to the interface between tendon and screw and between screw and bone. The specimen was placed in an MTS 858 BIONIX Test System (MTS Systems, Eden Prairie, MN) with a 1,500-lb load cell. The tibia was potted in methyl-methacrylate and mounted in a custom-designed fixture attached to the base of the testing machine. This allowed the tensile load to be applied to the graft in line with the bone tunnel. The tendon was gripped in a specially designed cryogrip with dry ice. The cryogrip was fixed to the load cell, which in turn was connected to the actuator of the MTS machine. A linear extensometer was attached to the proximal tibia and the cryogrip to measure the displacement of the tendon. A 50-N preload was applied, and peak load at failure (in newtons) and stiffness (in newtons per millimeter) were measured and recorded. Peak load was determined from the load-displacement curve. Stiffness was calculated by measuring the slope from the linear portion of the curve.

After mechanical testing, the specimens were examined macroscopically to determine the failure patterns. This was categorized as complete or partial pullout (i.e., the tendon failed inside the bone tunnel) or no pullout (i.e., the tendon ruptured proximal to, or outside of, the bone tunnel) in each treatment group.

Histologic Analysis

The remaining 12 stifles were used for histologic analysis after the interference screws were removed, because we hypothesized that it would be difficult to keep the interference screw in situ when the histologic specimen was cut into 100- μ m-thick sections for staining. The specimens were fixed in neutral-buffered 10% formalin. The tibia was first sectioned sagittally into a lateral one-third portion of the bone tunnel

TABLE 1. *Semiquantitative Grading Scale for Tendon-Bone Healing in Bone Tunnel*

	Description
New bone in tendon graft	
Grade 0	None
Grade 1	1 site
Grade 2	2-3 sites
Grade 3	≥ 4 sites
Mesenchymal cell density at interface	
Grade 0	No or minimal
Grade 1	Mild
Grade 2	Moderate
Grade 3	High

(entry site) and a medial two-thirds portion of the bone tunnel. The lateral one third of the tunnel was sectioned in the coronal plane through the center of the tunnel's axis. The medial two thirds of the bone tunnel was cut into 3 equal sections of the tunnel in the sagittal plane. The decalcified specimens were embedded in paraffin and then stained with H&E and Masson trichrome for the evaluation of tendon-to-bone healing. A modified semiquantitative scale, based on a previous study, was used to evaluate tendon-bone healing (Table 1).²⁴ The sections from each specimen were examined by 3 senior researchers blinded to group assignments, and the mean scores of the 3 researchers were used for statistical comparisons.

Statistical Analysis

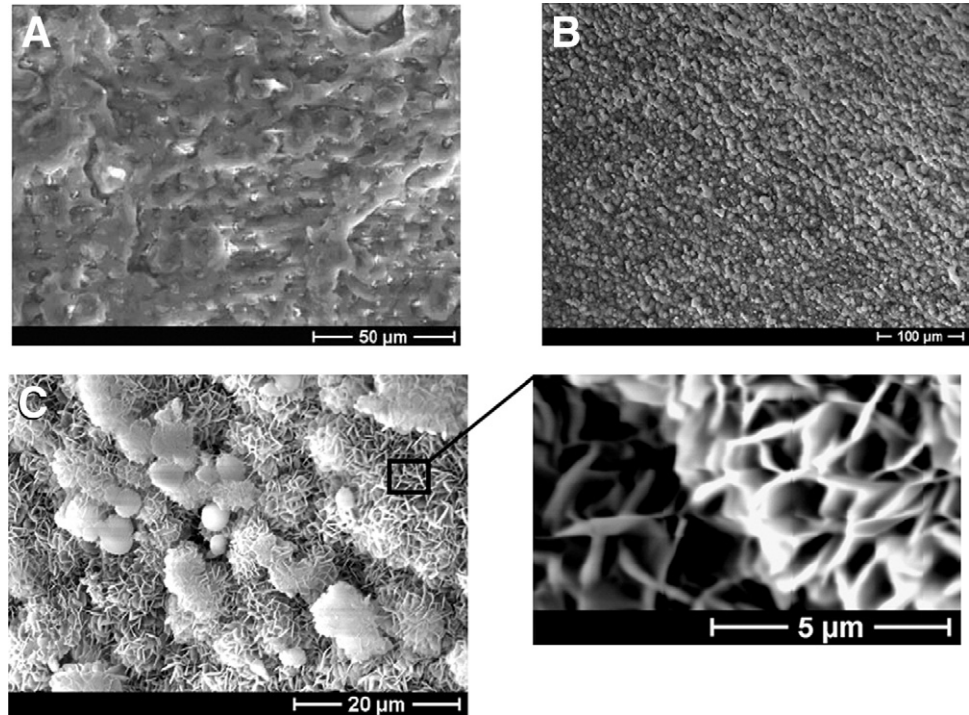
The Student paired *t* test was used for statistical analysis for mechanical testing data between the 2 treatment groups. A Fisher exact test was used to compare tendon pullout failure patterns between the 2 groups. Comparison of the histologic subjective scores between the treatment groups was performed by the Wilcoxon rank sum test. Differences were considered to be significant at a probability level of 95% ($P < .05$). All statistical analyses were performed with a commercially available software program (SAS, version 8e; SAS, Cary, NC).

RESULTS

Formation of Mineral Coatings on BIORCI Screws

Incubation of surface-hydrolyzed BIORCI interference screws in mSBF for 10 days resulted in growth of a continuous mineral coating on the surface (Figs 1A and 1B). The coating was similar in structure and

FIGURE 1. Scanning electron micrographs of surface of a BIORCI bone screw (A) before mineral coating and (B) after mineral coating. (C) Higher-resolution scanning electron micrographs of mineral coating, showing plate-like nanostructure.



composition to coatings we have grown previously on other biodegradable polymer materials (Fig 1C).¹⁹⁻²¹

Peptide Binding and Release Kinetics

The linkBMP-2 molecule bound efficiently to the surface of mineral-coated BIORCI screws, and the binding was dependent on the solution concentration of linkBMP-2 (Fig 2A). The binding curve reached a plateau at approximately 4 mg/mL of linkBMP-2 in

solution. The cumulative release of linkBMP-2 measured in vitro was gradual and sustained over time, and over 80% of the initially bound linkBMP-2 was released during a 6-week time frame in vitro (Fig 2B).

Implantation of Interference Screws

All sheep survived through the study without significant complications. In the linkBMP-2-coated interference screw group, all tendons failed outside of

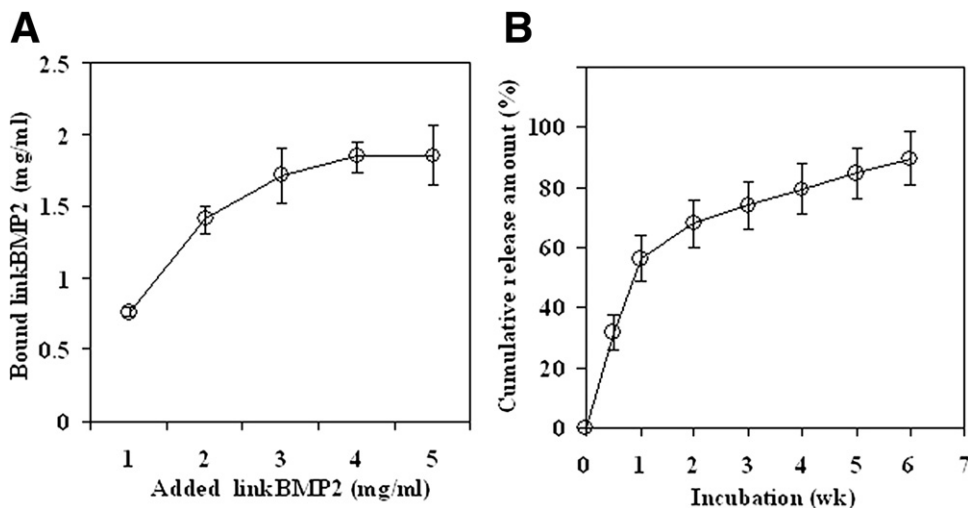


FIGURE 2. (A) Binding of fluorescein-labeled linkBMP-2 peptide to mineral-coated BIORCI screws. (B) Kinetics of linkBMP-2 peptide release in vitro.

the tunnel without pullout, whereas in the uncoated group, 2 tendons failed by partial pullout and 6 failed outside of the tunnel without pullout. There was no significant difference in the failure pattern between the 2 groups ($P = .52$).

Peak load at failure in the linkBMP-2-coated interference screw group (mean \pm SD, 449.3 \pm 84.7 N) was slightly but not significantly increased when compared with the uncoated group (421.0 \pm 61.8 N) ($P = .22$) (Table 2, available at www.arthroscopyjournal.org). Stiffness in the linkBMP-2-coated interference screw group (157.3 \pm 39.6 N/mm) also had a trend toward being greater than that in the uncoated group (140.6 \pm 20.3 N/mm), though this was not significant ($P = .12$). Histologic analysis showed that the tendons in the linkBMP-2-coated interference screw group (median, 5.5; range, 2.0 to 6.0) had significantly greater scores than the uncoated group (median, 2.0; range, 1.0 to 4.0) ($P < .05$) (Fig 3; Table 3, available at www.arthroscopyjournal.org). In the linkBMP-2-coated interference screw group, mesenchymal cells were present at the interface between screw and tendon, whereas these cells were not present in the uncoated group.

DISCUSSION

The results of this study showed that BIORCI interference screws can be successfully coated with a continuous inorganic layer and that the engineered

linkBMP-2 molecule bound efficiently to the surface of mineral-coated BIORCI screws. Over 80% of the initially bound linkBMP-2 was released during a 6-week time frame in vitro. In vivo results of this study showed that there were no significant differences in the failure pattern and mechanical properties between the linkBMP-2-coated and uncoated groups. Histologic analysis showed that the linkBMP-2-coated group had better histologic scores than the uncoated group.

The sheep model has been widely used for evaluating tendon-bone healing by scientific investigators.^{5,24-28} Sheep were selected for this study because their bone density and weight are similar to humans.²⁹ Pena et al.⁶ reported that bone density had an influence on determining peak loads at failure in human cadaveric specimens, so the use of sheep specimens can help to minimize specimen-related bias.

As reported in previous studies, several researchers had used this current model for evaluating the healing of a tendon graft in a bone tunnel by placing an LDE tendon in an extra-articular tunnel in the proximal metaphysis of an animal tibia.^{5,22} One advantage of this extra-articular model is that it avoids variables associated with intra-articular ACL graft positioning and tensioning.^{11,30} Another advantage is that this model allows the testing of 1 site of fixation, thus avoiding the difficulties in determining the strength and stiffness of 1 site of fixation when 2 sites of

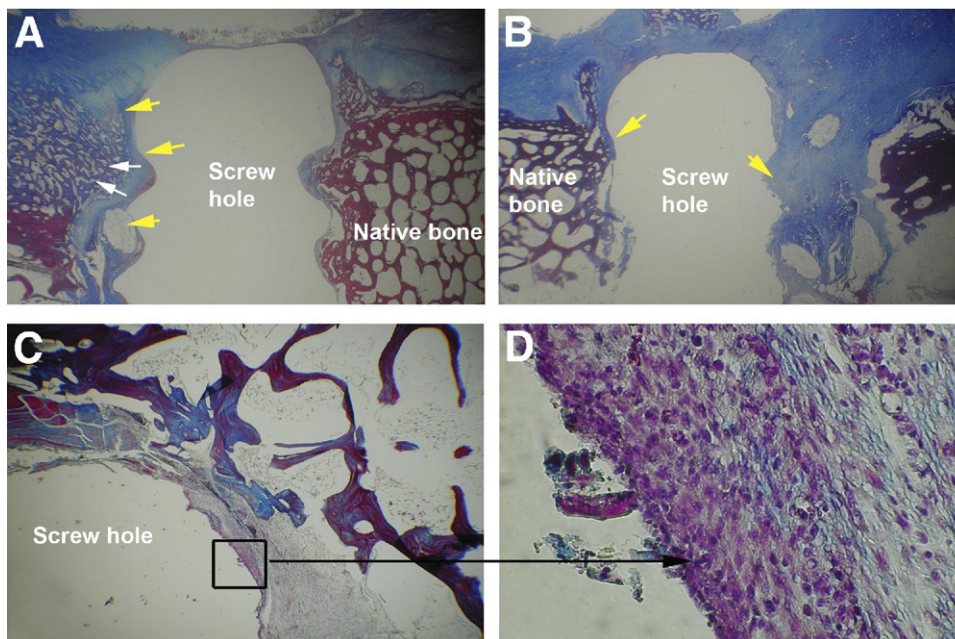


FIGURE 3. Histologic images showing LDE tendon (yellow arrows) in bone tunnel with interference screw removed. (A) Screw with linkBMP-2 coating. White arrows indicate new bone formation. (B) Screw without coating (original magnification $\times 1$). (C, D) The specified area (black square) of the LDE tendon in the bone tunnel of the linkBMP-2 coating group showed the presence of mesenchymal cells at the interface between screw and tendon (black arrow) (original magnification $\times 20$ in C and $\times 100$ in D).

fixation are tested simultaneously, as in an ACL reconstruction.³¹

A variety of clinical methods have been developed for controlled growth factor release. The most common methods involve encapsulation of growth factors within naturally derived materials, such as bioabsorbable collagen gels and sponges.¹² These approaches use materials that are amenable to clinical use and have therefore become the standard for delivery of BMP-2 and bone morphogenetic protein 7 to promote long bone healing, spine fusion, and dental bone regeneration. However, these current carrier materials are not appropriate for load-bearing applications, and the release kinetics of growth factors are suboptimal, resulting in a need to deliver superphysiologic doses—on the order of milligrams of protein per implant. The consequences of suboptimal growth factor delivery kinetics can include osteolysis,³² increased host response,³³ and tissue formation in undesired locations.¹⁴ Therefore there is a need to develop more sophisticated, clinically relevant strategies for growth factor delivery. The approach described in this report is advantageous in that the biologically active agent can be incorporated into the surface of an implant material. The general concept of decoupling bulk implant properties from surface biological activity could be useful in a variety of orthopaedic applications.

Rigid interference screw fixation in the tendon/ligament reconstruction relates to several factors such as screw length, screw diameter, thread shape, screw divergence, and gap size (tunnel-graft diameter).^{1,34-36} Scranton et al.³⁷ reported that incorporation of the graft involved neochondrification, neo-ossification, and Sharpey fibers, which had been identified as early as 6 weeks in a sheep model. In our study the time for over 80% linkBMP-2 release in vitro was 6 weeks. Therefore, although our study did not show a significant difference in mechanical properties between the linkBMP-2-coated and uncoated groups, the effects on healing may be more significant when explored at later time points.

Histologic analysis showed that the presence of linkBMP-2 on the interference screw led to an increased density of mesenchymal cells at the interface between the screw and LDE tendon, and this did not occur in the uncoated group. Although the fate of these mesenchymal cells could not be defined because of the short-term time frame of the study, this finding showed that the interference screw coated with growth factors may be a possible option for enhancing tendon-bone healing. This linkBMP-2 coating may be

useful as a component of other bone healing approaches, such as application of this coating on the surface of metal prostheses for total hip or total knee replacement.

Several limitations of this study need to be discussed. First, this study tested the linkBMP-2-coated interference screw under extra-articular conditions. The same outcome may not be applicable to intra-articular conditions, where joint fluid and active ligament/tendon loading occur. Second, the linkBMP-2-coated interference screw was evaluated in the tibia in this study; if it is tested in a femoral site, different outcomes may result because of different bone density. Third, the results from this quadruped animal model may not be applicable to humans because of different weight-bearing conditions. Fourth, 2 bioactive materials (hydroxyapatite and linkBMP-2) were assessed simultaneously, and thus it is not possible to determine the individual effect of either material. Fifth, a 6-week time period may not be long enough for evaluating the results of this study. Longer-term studies need to be performed in the future.

CONCLUSIONS

We found that linkBMP-2 can be bound onto a mineral-coated BIORCI interference screw surface and subsequently released from the screw surface in a sustained manner. The histologic result of this study showed that the linkBMP-2-coated interference screw significantly improved the histologic scores of early tendon-bone healing; however, mechanical testing did not show significant differences between the linkBMP-2-coated group and the uncoated group in this sheep model.

Acknowledgment: The authors thank Dimitrije Bogunovic, Tina Tsai, Vicki Kalcheur, and Hirohito Kobayashi for their technical assistance.

REFERENCES

1. Weiler A, Hoffmann RF, Siepe CJ, Kolbeck SF, Sudkamp NP. The influence of screw geometry on hamstring tendon interference fit fixation. *Am J Sports Med* 2000;28:356-359.
2. Brand J Jr, Weiler A, Caborn DN, Brown CH Jr, Johnson DL. Graft fixation in cruciate ligament reconstruction. *Am J Sports Med* 2000;28:761-774.
3. Harvey A, Thomas NP, Amis AA. Fixation of the graft in reconstruction of the anterior cruciate ligament. *J Bone Joint Surg Br* 2005;87:593-603.
4. Caborn DN, Coen M, Neef R, Hamilton D, Nyland J, Johnson DL. Quadrupled semitendinosus-gracilis autograft fixation in the femoral tunnel: A comparison between a metal and a

- bioabsorbable interference screw. *Arthroscopy* 1998;14:241-245.
5. Singhatat W, Lawhorn KW, Howell SM, Hull ML. How four weeks of implantation affect the strength and stiffness of a tendon graft in a bone tunnel: A study of two fixation devices in an extraarticular model in ovine. *Am J Sports Med* 2002;30:506-513.
 6. Pena F, Grontvedt T, Brown GA, Aune AK, Engebretsen L. Comparison of failure strength between metallic and absorbable interference screws. Influence of insertion torque, tunnel-bone block gap, bone mineral density, and interference. *Am J Sports Med* 1996;24:329-334.
 7. Thaanat M, Nourissat G, Gaudin P, Beaufile P. Tibial plateau fracture after anterior cruciate ligament reconstruction: Role of the interference screw resorption in the stress riser effect. *Knee* 2006;13:241-243.
 8. Kohn D, Rose C. Primary stability of interference screw fixation. Influence of screw diameter and insertion torque. *Am J Sports Med* 1994;22:334-338.
 9. Anderson K, Seneviratne AM, Izawa K, Atkinson BL, Potter HG, Rodeo SA. Augmentation of tendon healing in an intra-articular bone tunnel with use of a bone growth factor. *Am J Sports Med* 2001;29:689-698.
 10. Martinek V, Latterman C, Usas A, et al. Enhancement of tendon-bone integration of anterior cruciate ligament grafts with bone morphogenetic protein-2 gene transfer: A histological and biomechanical study. *J Bone Joint Surg Am* 2002;84:1123-1131.
 11. Rodeo SA, Suzuki K, Deng XH, Wozney J, Warren RF. Use of recombinant human bone morphogenetic protein-2 to enhance tendon healing in a bone tunnel. *Am J Sports Med* 1999;27:476-488.
 12. Geiger M, Li RH, Friess W. Collagen sponges for bone regeneration with rhBMP-2. *Adv Drug Deliv Rev* 2003;55:1613-1629.
 13. Li RH, Wozney JM. Delivering on the promise of bone morphogenetic proteins. *Trends Biotechnol* 2001;19:255-265.
 14. Shields LB, Raque GH, Glassman SD, et al. Adverse effects associated with high-dose recombinant human bone morphogenetic protein-2 use in anterior cervical spine fusion. *Spine* 2006;31:542-547.
 15. Liu Y, Enggist L, Kuffer AF, Buser D, Hunziker EB. The influence of BMP-2 and its mode of delivery on the osteoconductivity of implant surfaces during the early phase of osseointegration. *Biomaterials* 2007;28:2677-2686.
 16. Sumner DR, Turner TM, Urban RM, Virdi AS, Inoue N. Additive enhancement of implant fixation following combined treatment with rhTGF-beta2 and rhBMP-2 in a canine model. *J Bone Joint Surg Am* 2006;88:806-817.
 17. Sachse A, Wagner A, Keller M, et al. Osteointegration of hydroxyapatite-titanium implants coated with nonglycosylated recombinant human bone morphogenetic protein-2 (BMP-2) in aged sheep. *Bone* 2005;37:699-710.
 18. Saito A, Suzuki Y, Ogata S, Ohtsuki C, Tanihara M. Activation of osteo-progenitor cells by a novel synthetic peptide derived from the bone morphogenetic protein-2 knuckle epitope. *Biochim Biophys Acta* 2003;1651:60-67.
 19. Murphy WL, Mooney DJ. Bioinspired growth of crystalline carbonate apatite on biodegradable polymer substrata. *J Am Chem Soc* 2002;124:1910-1917.
 20. Murphy WL, Simmons CA, Kaigler D, Mooney DJ. Bone regeneration via a mineral substrate and induced angiogenesis. *J Dent Res* 2004;83:204-210.
 21. Murphy WL, Hsiong S, Richardson TP, Simmons CA, Mooney DJ. Effects of a bone-like mineral film on phenotype of adult human mesenchymal stem cells in vitro. *Biomaterials* 2005;26:303-310.
 22. Lu Y, Markel MD, Nemke B, Shawn W, Graf B. Comparison of single- versus double-tunnel tendon-to-bone healing in an ovine model: A biomechanical and histological analysis. *Am J Sports Med* 2009;37:512-517.
 23. Greis PE, Burks RT, Bachus K, Luker MG. The influence of tendon length and fit on the strength of a tendon-bone tunnel complex. A biomechanical and histologic study in the dog. *Am J Sports Med* 2001;29:493-497.
 24. Walsh WR, Cotton NJ, Stephens P, et al. Comparison of poly-L-lactide and polylactide carbonate interference screws in an ovine anterior cruciate ligament reconstruction model. *Arthroscopy* 2007;23:757-765, 765.e1-2.
 25. Goradia VK, Rochat MC, Grana WA, Rohrer MD, Prasad HS. Tendon-to-bone healing of a semitendinosus tendon autograft used for ACL reconstruction in a sheep model. *Am J Knee Surg* 2000;13:143-151.
 26. Goradia VK, Rochat MC, Kida M, Grana WA. Natural history of a hamstring tendon autograft used for anterior cruciate ligament reconstruction in a sheep model. *Am J Sports Med* 2000;28:40-46.
 27. Weiler A, Hoffmann RF, Bail HJ, Rehm O, Sudkamp NP. Tendon healing in a bone tunnel. Part I: Histologic analysis after biodegradable interference fit fixation in a model of anterior cruciate ligament reconstruction in sheep. *Arthroscopy* 2002;18:124-135.
 28. Weiler A, Peine R, Pashmineh-Azar A, Abel C, Sudkamp NP, Hoffmann RF. Tendon healing in a bone tunnel. Part II: Biomechanical results after biodegradable interference fit fixation in a model of anterior cruciate ligament reconstruction in sheep. *Arthroscopy* 2002;18:113-123.
 29. Campbell AW, Bain WE, McRae AF, et al. Bone density in sheep: Genetic variation and quantitative trait loci localisation. *Bone* 2003;33:540-548.
 30. Rodeo SA, Amoczky SP, Torzilli PA, Hidaka C, Warren RF. Tendon-healing in a bone tunnel. A biomechanical and histological study in the dog. *J Bone Joint Surg Am* 1993;75:1795-1803.
 31. Magen HE, Howell SM, Hull ML. Structural properties of six tibial fixation methods for anterior cruciate ligament soft tissue grafts. *Am J Sports Med* 1999;27:35-43.
 32. McClellan JW, Mulconrey DS, Forbes RJ, Fullmer N. Vertebral bone resorption after transforaminal lumbar interbody fusion with bone morphogenetic protein (rhBMP-2). *J Spinal Disord Tech* 2006;19:483-486.
 33. Sigurdsson TJ, Nygaard L, Tatakis DN, et al. Periodontal repair in dogs: Evaluation of rhBMP-2 carriers. *Int J Periodontics Restorative Dent* 1996;16:524-537.
 34. Selby JB, Johnson DL, Hester P, Caborn DN. Effect of screw length on bioabsorbable interference screw fixation in a tibial bone tunnel. *Am J Sports Med* 2001;29:614-619.
 35. Fineberg MS, Zarins B, Sherman OH. Practical considerations in anterior cruciate ligament replacement surgery. *Arthroscopy* 2000;16:715-724.
 36. Steenlage E, Brand JC Jr, Johnson DL, Caborn DN. Correlation of bone tunnel diameter with quadrupled hamstring graft fixation strength using a biodegradable interference screw. *Arthroscopy* 2002;18:901-907.
 37. Scranton PE Jr, Lanzer WL, Ferguson MS, Kirkman TR, Pflaster DS. Mechanisms of anterior cruciate ligament neovascularization and ligamentization. *Arthroscopy* 1998;14:702-716.

TABLE 2. *Histological Semiquantitative Scores for Tendon-Bone Healing in Bone Tunnel (6 Sheep [12 Stifles])*

Sheep No.	Treatment	Score
221	linkBMP-2	6
220	linkBMP-2	5
61	linkBMP-2	6
54	linkBMP-2	4
53	linkBMP-2	6
60	linkBMP-2	2
221	Uncoated	1
220	Uncoated	1
61	Uncoated	4
54	Uncoated	2
53	Uncoated	4
60	Uncoated	2

TABLE 3. *Mechanical Testing Data for Peak Load and Stiffness (8 Sheep [16 Stifles])*

Sheep No.	Treatment	Peak Load (N)	Stiffness (N/mm)
213	linkBMP-2	452	164
211	linkBMP-2	491	178
58	linkBMP-2	433	137
56	linkBMP-2	527	187
55	linkBMP-2	291	94
57	linkBMP-2	531	208
52	linkBMP-2	505	179
59	linkBMP-2	364	111
213	Uncoated	385	147
211	Uncoated	399	138
58	Uncoated	399	121
56	Uncoated	514	171
55	Uncoated	318	107
57	Uncoated	489	146
52	Uncoated	419	159
59	Uncoated	445	136